Adsorption and Cyclotrimerization Kinetics of C2H2 at a Cu(110) Surface

ARTICLE *in* THE JOURNAL OF PHYSICAL CHEMISTRY C · APRIL 2012

Impact Factor: 4.77 · DOI: 10.1021/jp300514f

THE JOURNAL OF PHYSICAL CHEMISTRY C

Article

pubs.acs.org/JPCC

Adsorption and Cyclotrimerization Kinetics of C_2H_2 at a Cu(110) Surface

H. Öberg,[†] Y. Nestsiarenka,[†] A. Matsuda,[†,‡] J. Gladh,[†] T. Hansson,[†] L. G. M. Pettersson,[†] and H. Öström*,[†]

[†]Department of Physics, AlbaNova University Center, Stockholm University, SE-106 91 Stockholm, Sweden

[‡]Research Center for Materials Science, Nagoya University, Furo, Chikusa, Nagoya, Aichi 464-8602, Japan

Supporting Information

ABSTRACT: The kinetics of acetylene adsorption and cyclotrimerization was studied by vibrational sum-frequency generation spectroscopy (SFG) and density functional theory (DFT) calculations. At low temperature, SFG shows two resonances corresponding to acetylene adsorbed in two different sites. Upon heating, two new vibrational resonances appear. We interpret these resonances as being due to C_2H_2 island formation and adsorbed C_4H_4, which is the intermediate in the subsequent cyclotrimerization reaction to form benzene. A kinetic model is applied, which allows determination of the relevant activation barriers. The barrier for C_2H_2 diffusion is determined to be 43 ± 1 kJ/mol. The activation barrier for formation of the C_4H_4 intermediate is found to be 84 ± 6 kJ/mol and the barrier for benzene formation 5 ± 3 kJ/mol lower. Barriers to diffusion and formation of C_4H_4 and C_6H_6 obtained from DFT calculations are in quantitative agreement with the experiments once the locally high coverage in C_2H_2 islands is included.

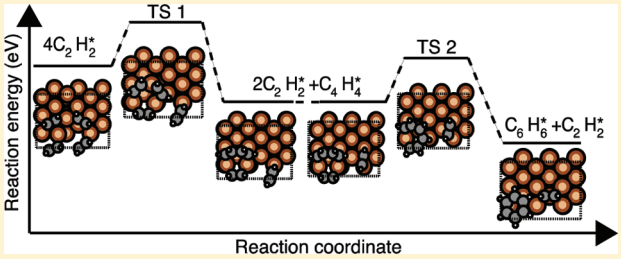

INTRODUCTION

Adsorption and reaction of small molecules at metal surfaces have for a long time worked as model systems for heterogeneous catalysis. Acetylene cyclotrimerization has been observed and studied at various surfaces,[1−13] especially on palladium on which benzene formation may occur also through reaction of acetylene with vinylidene. This is not the case for copper, which suggests interesting underlying differences in the bonding of hydrocarbons to transition metal surfaces. Adsorption of unsaturated hydrocarbons in general can be well described within the Dewar−Chatt−Duncanson (DCD) model,[14,15] where the frontier orbitals of the molecule interact with the frontier orbitals of the metal surface, leading to a rather large rehybridization and bond elongation of the bonding C atoms.[16−23] The bonding can alternatively be described in the spin-uncoupling picture[24] in which the π-donation and π^* back-donation of the DCD model is viewed as a $\pi \rightarrow \pi^*$ molecular excitation, allowing the energetics in the bond formation to be analyzed. This is also true in the case of C_2H_2 adsorbed at Cu(110), where the C−C bond elongates and the C−H bonds bend up rendering an essentially sp^2 hybridized molecule[25] in a geometry similar to the gas phase excited triplet state.[24]

At the Cu(110) surface, C_2H_2 adsorbs into two different adsorption sites, with different C−C axis orientation.[25] Scanning tunneling microscopy (STM) experiments have shown different types of C_2H_2 clusters already at low temperature and coverage.[26] In the same study, inelastic electron tunneling spectroscopy (IETS) was used to observe electron-induced migration, and the hopping was determined to proceed via excitation of C−H stretch vibrations.

Acetylene cyclotrimerization has, as mentioned above, received the most attention at Pd surfaces, where the kinetics as well as adsorption of the reactant and intermediate species have been characterized and the reaction was found to proceed in a purely associative pathway with an adsorbed tilted C_4H_4 intermediate.[2] At Pd surfaces, desorption of C_6H_6 was found to be the rate-limiting step. The cyclotrimerization reaction also occurs at Cu surfaces. In particular, Cu(110) shows a high selectivity toward cyclotrimerization of C_2H_2 under UHV conditions at rather low temperature. Upon heating, up to 85% of the adsorbed C_2H_2 molecules form C_6H_6 on Cu(110) around 325 K.[2] The reaction occurs also at the other low-index Cu surfaces but with lower selectivity. At the Cu(100) surface, 30% of the acetylene converts to benzene[3] and around 5% at Cu(111).[4] Like at Pd surfaces, the reaction proceeds via an associative path, but unlike Pd the cyclotrimerization is reaction-rate limited at Cu surfaces.[2]

The bonding of benzene to Cu(110) was investigated in ref 24, and two adsorption states were found with an inverted boat form more stable than the physisorbed species; both however showed a slight bending up of the hydrogens. The inverted boat form corresponds to the quinoid triplet excited state of benzene, which localizes the two unpaired spins in para

Received: January 16, 2012
Revised: April 9, 2012
Published: April 9, 2012

   dx.doi.org/10.1021/jp300514f | J. Phys. Chem. C 2012, 116, 9550−9560

position to form two σ-bonds to the surface. This would give a characteristic signal in X-ray absorption spectroscopy (XAS) which is observed when benzene is adsorbed from the gas phase on Ni, Mo, and Pt surfaces but not on Cu(110).[27] In ref 24, it was suggested that the involvement of the excited triplet state in the inverted boat form could lead to a barrier when adsorbing from the gas phase, and it was speculated that this more stable form could be generated in the cyclotrimerization reaction. Due to the short-lived nature of the adsorbed C_4H_4 and C_6H_6, these have, however, not been detected at the Cu surface during reaction.

Benzene formation also occurs upon heating of chlorinated C_2H_2 compounds on Cu(110).[28−30] This reaction proceeds via initial dissociation of C−Cl bonds followed by cyclotrimerization of the resulting C_2H_2 species, with the rate of cyclotrimerization limited by desorption. Cyclotrimerization was also observed for larger hydrocarbons at the Cu(110) surface.[31]

Infrared-visible sum-frequency generation (SFG) spectroscopy[32] provides a highly surface-sensitive vibrational spectroscopy probe, with reasonably high resolution and a large signal to background ratio. The spectroscopy can be used in broadband mode[33] where an entire spectrum is recorded for every laser shot, which makes data acquisition fast and is useful to study the thermal evolution of adsorbed species during a reaction.[34,35]

In the present paper, we present a vibrational SFG study of the C_2H_2 adsorbate system, which provides insights into the thermal evolution of the adsorbed C_2H_2 and the kinetics of C_2H_2 cyclotrimerization at the Cu(110) surface. We observe an intermediate C_4H_4 species and provide details on the kinetics of the reaction. Complementary density functional theory (DFT) calculations on the C_2H_2 adsorption and cyclotrimerization provide detailed insight into the reaction mechanism.

METHODS

Experiment. The experiments were performed in an ultrahigh vacuum (UHV) chamber with a base pressure below 1×10^{-10} Torr, which is combined with a high-power femtosecond Ti:sapphire laser system.

The Cu(110) crystal was cleaned in situ by cycles of Ar ion sputtering at 1 kV, followed by resistive annealing to 870 K until reproducible CO TPD and vibrational data in agreement with the literature[36,37] were obtained and LEED showed a sharp 1×1 pattern. The LEED optics is a two-grid erLEED100 from SPECS. For the temperature-dependent measurements, the kinetic energy of the electrons was set to 100 eV. C_2H_2, $C_4H_4Cl_2$, or C_6H_6 was dosed via a collimated channel plate doser at a sample temperature of 105 K, which reduces the gas load in the UHV chamber as well as wall reactions. The dose was controlled by varying the dosing time while keeping the background pressure constant in the gas line.

A femtosecond laser amplifier system, providing pulses with a temporal width of 50 fs and up to 2.5 mJ pulse energy at 800 nm with a repetition rate of 1 kHz combined with an OPG/OPA stage with a noncollinear difference frequency generation (nDFG) stage, was used. For the present experiment, the nDFG was set to 3000 cm^{-1}, which yielded an IR spectrum of width ~450 cm^{-1}, to overlap with the C−H stretching vibrational range. These pulses were used together with spectrally narrowed 800 nm pulses to perform broadband vibrational SFG spectroscopy.[33] Sum-frequency generation is a second-order nonlinear optical process where two incident light waves are combined to yield a wave with the sum-frequency of the incoming waves.[38] Both energy and momentum are conserved in this process, which gives rise to a powerful selection rule stating that within the dipole approximation the sum-frequency wave can only be created if inversion symmetry in the system is broken. This selection rule makes the process highly sensitive to surface phenomena, and the sum-frequency process can be described by the second-order nonlinear susceptibility tensor. If one of the incoming waves in addition is spectrally overlapped with adsorbate vibrations, a resonant enhancement can occur, and vibrational spectroscopy can be performed.[32] The SFG signal was spectrally resolved and recorded using an optical spectrograph equipped with an intensified CCD camera for efficient detection. The experimental frequency resolution is limited by the spectrometer resolution and spectral width of the 800 nm up-conversion pulses and was typically set to ~8 cm^{-1} full width at half-maximum (fwhm). To obtain the temperature-dependent data, the intensity of the up-conversion light was increased, and the spectral resolution was reduced to 12 cm^{-1}. The up-conversion frequency was subtracted from the observed frequency, and the spectra are presented on the vibrational energy scale. The spectra were frequency calibrated in the infrared using the known vibrational frequency of adsorbed CO.[36]

Typical pulse energies were around 5 μJ each for the infrared and up-conversion pulses. The beam diameter of the up-conversion pulse at the sample was around 500 μm, while the mid-infrared ones were slightly larger.

The SFG spectral intensity can typically be well described by the square of the sum of a nonresonant susceptibility and a number of vibrational resonances, where the relative phases are taken into account.[39] The spectra were fitted using this model, and the nonresonant background, as measured on the clean sample, was taken as a spectral profile of the infrared pulses. The phase shift between resonant and nonresonant contributions typically leads to an asymmetric line shape and can give rise to a small shift between the resonance position and the peak maximum.

Theory. All calculations were done using GPAW[40,41] which is a real-space, grid-based, all-electron density functional theory (DFT) code implemented in the projector-augmented wave (PAW) formalism.[42] In this approach we employ pseudowave functions with smooth behavior near the core inside the augmentation spheres. What makes this method different in comparison to, e.g., the pseudopotential approach is the possibility of reconstructing the true wave function through addition and subtraction of atomic corrections which thus allows transforming to an explicit frozen-core all-electron description of the system of interest. We performed the calculations using the RPBE exchange-correlation (XC) functional, which is the revision suggested by Hammer et al.[43] to improve adsorption energetics compared to the functional originally developed by Perdew, Burke, and Ernzerhof,[44] and with the grid spacing set to the default value of 0.2 Å. The Cu(110) surface was modeled with the GPAW-optimized Cu lattice parameter a = 3.643 Å compared to the experimental value 3.610 Å. Four-layer slab supercells were used containing up to 48 atoms and for which periodic boundary conditions were employed in each direction; in the surface normal direction, the slabs were separated by 14 Å of vacuum. To facilitate convergence, we used a Fermi smearing of 0.1 eV. The irreducible Brillouin zone was integrated using the standard Monkhorst−Pack scheme[45] with a $6 \times 6 \times 1$ k-point

dx.doi.org/10.1021/jp300514f | J. Phys. Chem. C 2012, 116, 9550−9560

mesh. Convergence of the chemisorption energy with respect to the *k*-point sampling was reached to within ~20 meV for the smallest supercell used in the study. Gas-phase acetylene was calculated in a 16 Å cubic cell at the Γ point without periodic boundary conditions. Frequencies were calculated using a finite difference approximation to the Hessian.

The binding energy of acetylene is calculated as the difference between the total energy of the chemisorbed species and the summed total energy of the clean slab and gas-phase acetylene: $E_{ads} = (E[nC_2H_2(ads)] - (E[Cu(110)\text{-slab}] + E[nC_2H_2(g)]))/n$, where n is the number of acetylene molecules adsorbed in the supercell.

We have calculated the reaction process at a surface coverage of 0.33 and 0.44 ML with respect to C_2H_2 where the cyclotrimerization proceeds via a C_4H_4 species in a first dimerization step. Diffusion was modeled at 0.25 and 0.11 ML of acetylene. Activation barriers for both the diffusion of acetylene and each of the steps in the cyclotrimerization to benzene were obtained using the Nudged-Elastic-Band (NEB) method[46] with at least six intermediate images allowed to simultaneously relax. We employed a smaller *k*-point sampling of 2 × 2 × 1 during these simulations. The Climbing-Image algorithm (CI-NEB) was activated after a few iterations to converge the transition state corresponding to the saddle point on the minimum energy path (MEP). In the NEB method, a path between initial reactants and product is mapped out by the intermediate images.

The effect of van der Waals interactions on the cyclotrimerization reaction as well as the adsorption energies was investigated for selected configurations by calculating single-point energies on the RPBE geometries using a self-consistent fast Fourier transform (FFT) implementation[47] of the vdW−DF functional.[48,49]

RESULTS

SFG Spectra. Figure 1 shows the SFG spectra around the region of the C−H stretch vibrational frequency for saturation coverage of C_2H_2/Cu(110). The nonresonant SFG background recorded for the clean sample is shown on the bottom and essentially shows the spectral shape of the broadband IR pulse, which is set to the frequency region spanning the range of the C−H stretching vibrations. The top spectrum was recorded for saturation coverage of C_2H_2 dosed at 110 K, for which a c(2 × 2) LEED pattern was detected. In addition to a nonresonant background, like the one for the clean sample, a pronounced resonant contribution is observed with maximum intensity at 2821 cm^{-1} together with a weaker resonant contribution at 2896 cm^{-1}, labeled #1 and #2, respectively. After resistively heating to 250 K at a ramping rate of 100 K/min and immediate subsequent cooling (flashing), we obtained the middle spectrum in Figure 1. The strong peak #1 at 2821 cm^{-1} shifts to 2808 cm^{-1} and its intensity decreases dramatically. Peak #2 at 2896 cm^{-1} shifts to 2889 cm^{-1} and grows, and a third peak (#3) appears at 2929 cm^{-1}. The spectra are consistent with previous inelastic electron tunneling spectroscopy (IETS)[26] data, which show a resonance at 350 meV (2823 cm^{-1}) for isolated C_2H_2 in perfect agreement with our resonance #1, as well as with EELS recorded for C_2H_2 adsorbed at low temperature. EELS, after heating to 280 K,[1,23] shows the C−H stretch resonance at 2880−2900 cm^{-1}, corresponding to peak #2 in our data. Peak #3 was not previously reported.

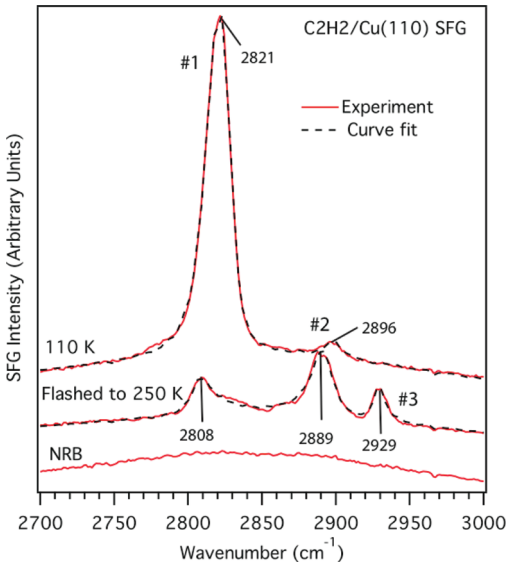

Figure 1. Top: SFG spectrum recorded for saturation coverage of C_2H_2 adsorbed at a Cu(110) surface at 110 K. Middle: Spectrum after flashing the sample to 250 K. Bottom: Nonresonant background (NRB) recorded for a clean Cu(110) surface.

The spectra were fitted using a model incorporating three resonances, which is the minimum required to get a good fit to the experiment. A single resonance does not provide a good fit to the low-frequency peak #1 in the low-temperature spectrum. It can, however, be fitted by two resonances located at 2816 and 2828 cm^{-1}, while the high-frequency resonance is reproduced by a single resonance at 2896 cm^{-1}. The need for two resonances to fit peak #1 suggests that the peak is not Lorentzian, presumably due to C_2H_2 molecules experiencing different interadsorbate interaction. The low-frequency peak #1 in the spectrum recorded after flashing can in contrast be fitted with a single resonance at 2808 cm^{-1}, while the high-frequency resonances appear at 2889 cm^{-1} (#2) and 2929 cm^{-1} (#3). At least part of the asymmetry of the 2808 cm^{-1} resonance can probably be attributed to resonance shifts due to differences in interadsorbate interaction. The 2929 cm^{-1} resonance has a fitted width of 9 cm^{-1} full-width at half-maximum, whereas the other resonances have a width around 12 cm^{-1}.

Structure. Previous XPS data,[25] as well as STM,[26] have shown the existence of two distinctly different adsorbate species at low temperature. According to STM all C_2H_2 adsorbate molecules adsorb aligned with the [001] direction of the Cu(110) surface, and the second species was assigned to adsorption in the long-bridge site, stabilized by intermolecular interactions. X-ray absorption spectroscopy (XAS) combined with density functional theory calculations, on the other hand, showed that one of the two species aligns along [001] in the 4-fold hollow site, and the other is lying down at the surface at an average angle of 35° from the [1-10] direction.[25] The XAS data of the latter species were, however, recorded at low temperature after flashing the sample to 260 K.

We have calculated vibrational frequencies for a number of different configurations to compare with the present SFG data, and we also present the corresponding chemisorption energies to give an indication of the relative stability of the respective configurations. To facilitate further discussions, we apply a similar notation as used in ref 25 where the species were denoted LBE (Low Binding Energy) and HBE (High Binding

dx.doi.org/10.1021/jp300514f | J. Phys. Chem. C 2012, 116, 9550−9560

Energy) according to their XPS binding energy; the adsorbate species aligned along the [001] surface direction are denoted LBE-h if adsorbed in a hollow site, LBE-b if aligned in the long-bridge site, and HBE if adsorbed asymmetrically, i.e., with an angle from the [001] direction (see Figure 2). We investigate

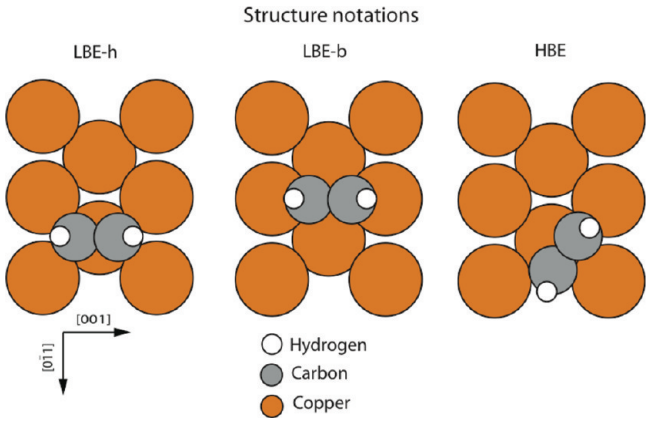

Figure 2. Structures of the LBE-h (low XPS binding energy adsorbed symmetrically in the hollow site), LBE-b (low XPS binding energy adsorbed symmetrically in the long-bridge site), and HBE (high XPS binding energy adsorbed asymmetrically in the hollow site) molecules.

the findings in the STM study,[26] in which isolated LBE-h acetylene molecules were observed as well as a LBE-b species stabilized by an intermolecular interaction with the LBE-h adsorbates, by calculating chemisorption energies of isolated LBE-h at 0.25 and 0.5 ML surface coverage, of LBE-b at 0.25 ML (at 0.5 ML no potential energy minimum could be found), and of LBE-h and LBE-b coadsorbed at a coverage of 0.33 ML. The results for the species aligned along the [001] direction, i.e., the LBE-h and LBE-b, are presented in Table 1.

Table 1. Vibrational Frequencies of the Symmetric C−H Stretch of Acetylene Species Adsorbed along the [001] Direction[a]

species	coverage (ML)	calcd vib. freq. (cm^{-1})	E_{ads} (eV)
LBE-h	0.50	2929 (2869)	−0.696
LBE-**h**/b	0.33	2951 (2892)	−0.700 (−1.120)
LBE-h/**b**	0.33	2972 (2912)	−0.420 (−1.120)
LBE-h	0.25	2963 (2904)	−0.698
LBE-b	0.25	2960 (2901)	−0.289

[a]LBE-h/b denotes C_2H_2 molecules coadsorbed in hollow (h) and bridge (b) sites. The bold font indicates the species for which the vibrational frequency is reported. The corresponding chemisorption energies per C_2H_2 are also shown. The number inside the parentheses gives, respectively, the scaled frequency (factor 0.98, see text) and the adsorption energy for both molecules in the cell where the adsorption energy of LBE-h is assumed independent of the LBE-b species.

The chemisorption energies indicate that isolated LBE-h adsorbates are more stable than the LBE-b species by ∼0.4 eV and that the stability of the former is independent of acetylene surface coverage (same energy value at 0.25 and 0.5 ML). Having a surface configuration in which the different symmetrically adsorbed LBE species are coadsorbed and assuming the adsorption energy of LBE-h remains constant in this mixed system increases the stability of LBE-b by ∼0.1 eV compared to isolated LBE-b molecules, which indicates a stabilizing intermolecular interaction in agreement with the STM measurements.[26]

Vibrational frequencies were computed using finite differences to build the Hessian and were calibrated against gas-phase acetylene for which we obtain 3441 (3374) cm^{-1} and 3348 (3289) cm^{-1} for the symmetric and antisymmetric CH stretch, respectively; experimental values[50] are given in parentheses. This would indicate a scaling factor of 0.98 between computed and actual frequencies which will be applied in the following and are given in parentheses.

We note a blue-shift in the computed symmetrical C−H stretch vibrational frequency of C_2H_2 molecules adsorbed in a long-bridge site (LBE-b) compared to that of acetylene adsorbed in a 4-fold hollow site (LBE-h) in the coadsorption system and to that of LBE-h at higher coverage. If we consider the isolated LBE-h species at 0.5 ML coverage, which gives rise to a c(2 × 2) pattern equivalent to the LEED results observed in the present study, and compare it with the LBE-b in the coadsorbed system, the vibrational frequency difference is obtained as ∼44 (43) cm^{-1}. This is similar to the results in Figure 1 recorded before flashing, where peak #2 is blue-shifted compared to peak #1, however by a larger amount, ∼75 cm^{-1}.

We have also calculated chemisorption energies and vibrational frequencies (see Table 2) of a number of different

Table 2. Vibrational Frequencies of the Asymmetric and Symmetric C−H Stretch of a Number of Different Configurations (See Figure 3) Containing Species Adsorbed Asymmetrically, With an Angle from the [1-10] Direction, Denoted HBE[a]

species	coverage (ML)	calcd vib. freq. (cm^{-1})	E_{ads} (eV)
A	0.33	2929 (2870)/2987 (2927)	−0.337
B	0.33	2918 (2860)/2953 (2892)	−0.539
C	0.25	-	−0.588
D	0.38	-	−0.464
E	0.33	-	−0.501
F	0.50	2935 (2876)/2999 (2939)	−0.201

[a]Vibrational frequencies are taken for the indicated molecule in Figure 3. The chemisorption energies for the HBE molecules are also shown; see the definition of the chemisorption energy in the main text. The number inside the parentheses gives the scaled frequency (factor 0.98, see text).

configurations (see Figure 3) containing asymmetrically adsorbed acetylene species, denoted HBE, which was reported in ref 25. For configurations B, C, D, and F all the molecules in the supercells are adsorbed asymmetrically and therefore classified as HBE. The chemisorption energy per HBE molecule for these configurations is thus simply defined as explained in the Methods section: $E_{ads}(\mathrm{HBE}) = (E[n\mathrm{C_2H_2(ads)}] - (E[\mathrm{Cu(110)\text{-}slab}] + E[n\mathrm{C_2H_2(g)}]))/n$, where n is the number of acetylene molecules adsorbed in the supercell. For configurations A and E, some of the molecules adsorbed in the supercells have an angle to the [1-10] direction very close to 90° (85−86°) which means we can classify them as LBE-h molecules. To isolate the chemisorption energy for the HBE species we subtract the adsorption energy of the LBE-h species, $E_{ads}(\mathrm{LBE\text{-}h}) = 0.7$ eV (see discussion earlier in the text), from the total chemisorption energy so that for these configurations we have $E_{ads}(\mathrm{HBE}) = (E[n\mathrm{C_2H_2(ads)}] - (E[\mathrm{Cu(110)\text{-}slab}] + E[n\mathrm{C_2H_2(g)}]) - mE[\mathrm{LBE\text{-}h}])/k$, where n is the number of molecules in the supercell, m the number of LBE-h molecules,

dx.doi.org/10.1021/jp300514f | J. Phys. Chem. C 2012, 116, 9550−9560

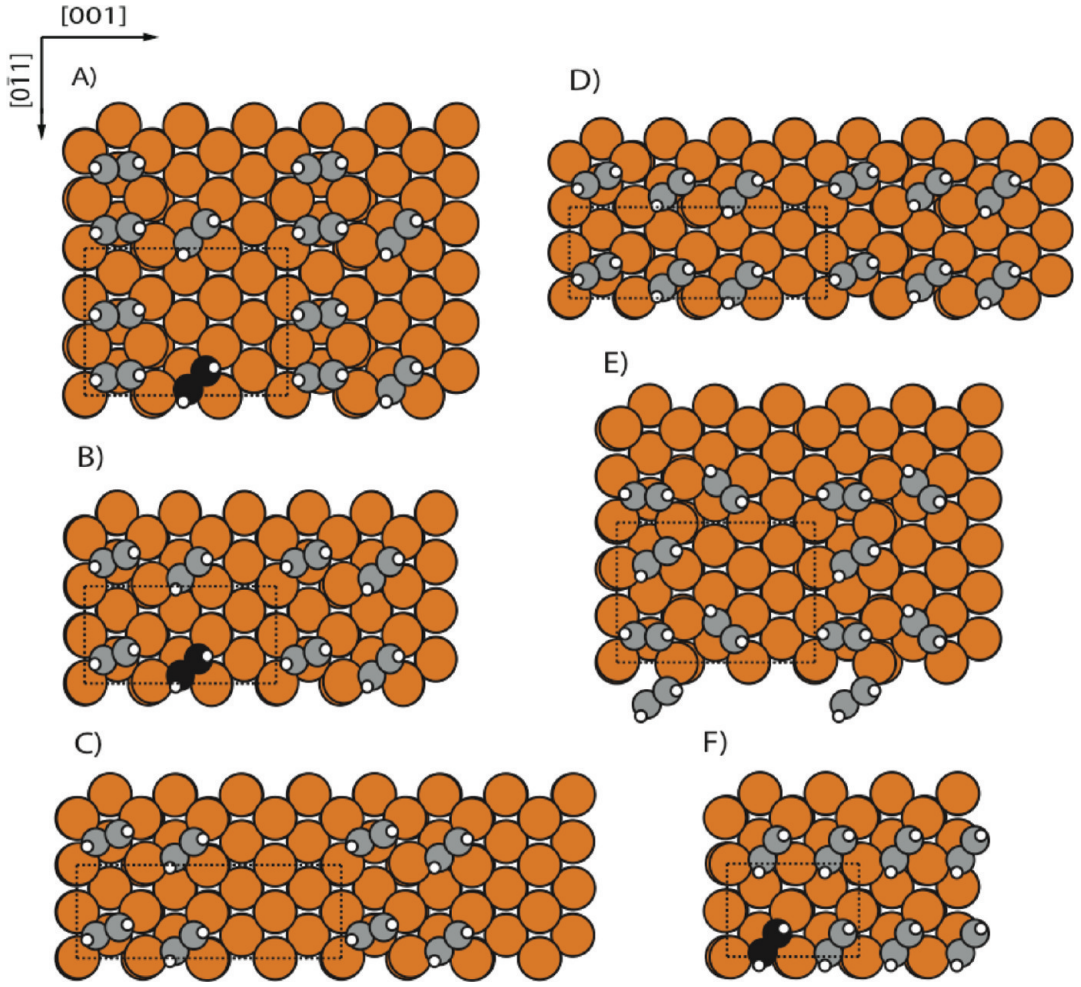

Figure 3. Six different configurations for which chemisorption energies and vibrational frequencies (black molecules only) are calculated. Coordinates are available in the Supporting Information.

and k the number of HBE species adsorbed in the cell. We note that the chemisorption energy per HBE molecule differs considerably depending on the local configuration. Comparing a situation where the HBE molecules are adsorbed in p(2 × 1) surface structure, configuration F in Figure 3, with the most stable configuration, C in the same figure, the adsorption energy differs by ∼0.4 eV, indicating that adsorbate−adsorbate interactions strongly affect the stability of the configurations containing asymmetrically adsorbed C_2H_2 molecules.

From the computed frequencies, we note that the difference between the asymmetric and the symmetric C−H stretch is rather sensitive to the environment that the acetylene in question experiences; it varies by ∼29 cm^{-1} when comparing the extreme cases. For configuration B, this difference is ∼35 cm^{-1}, in good agreement with the experimental difference of 40 cm^{-1} observed in Figure 1 between peaks #2 and #3 in the spectrum recorded after flashing the sample, but for the other configurations the difference is larger. We also observe a variation when considering the absolute positions of the vibrational frequencies of the C−H stretches. This can qualitatively, however, be correlated to the angle of the C−C axis to the [1-10] direction. Comparing the three configurations for which the vibrational frequencies have been calculated, A, B, and F, this angle varies from 85° down to 36° for the different molecules, an angular decrease that corresponds to a blue-shift of the symmetrical C−H stretch of ∼54 cm^{-1}. It is noteworthy that the angle for the adsorbates in F (36°), as well as the highlighted molecule in A (44°), compares well with the experimentally observed angle of ∼35°.[25]

Using this information we assign the 2821 cm^{-1} peak (#1) to the low-temperature species, the LBE-h, with its C−C axis in the surface plane and along the [001] surface direction. For such a symmetrically adsorbed species, we only expect the symmetric C−H stretch vibration to be SFG active. The symmetric adsorption site with hydrogen atoms flipped upward can also give a relatively large cross-section in SFG. The asymmetric stretch vibration will be inactive since it only gives rise to changes in the dipole moment in the surface plane that are efficiently screened by the metal surface. We assign peak #2 at 2896 cm^{-1} before flashing to the symmetric C−H stretch of a symmetrically adsorbed C_2H_2 species, which is compatible, e.g., with the long-bridge adsorbed C_2H_2, the LBE-b, suggested from STM.[26] Furthermore, we assign peaks #2 and #3 at 2889 and 2929 cm^{-1} after flashing to the asymmetrically adsorbed C_2H_2 species observed by XAS,[25] denoted HBE, for which, due to its asymmetry, two local C−H stretches can be SFG active. Alternatively, these resonances can originate from two different HBE species provided they have similar XPS binding energies.

Electron-induced hopping of isolated C_2H_2 molecules has been studied with STM and IETS,[26] and the 4-fold hollow site, associated with the vibrational resonance #1 at 2821 cm^{-1}, was found to be stable for isolated molecules also after energy

dx.doi.org/10.1021/jp300514f | J. Phys. Chem. C 2012, 116, 9550−9560

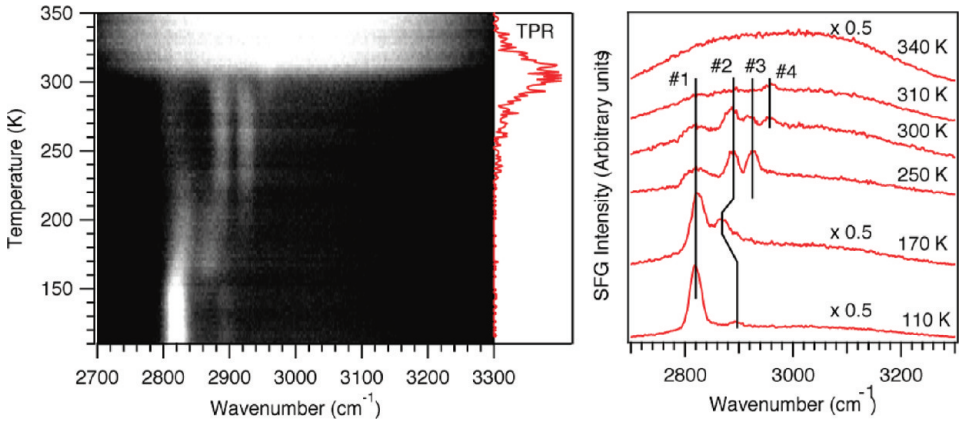

Figure 4. Left: False color plot showing the temperature dependence of SFG spectra from C_2H_2/Cu(110). Light parts indicate more and dark parts less intensity. Heating rate: 0.4 K/s. Middle: Benzene desorption signal from adsorbed C_2H_2. Right: Spectra around selected temperatures.

injection in the form of electrons that could cause hopping, i.e., where the C_2H_2 molecules migrate between equivalent sites without forming surface islands. This suggests that the most stable adsorption site for isolated molecules is the LBE-h site. At higher coverage, however, our experiment, as well as previously with core-level spectroscopies,[25] suggests that the HBE molecules, which predominate at high temperature, are more stable. Consequently, we conclude that these species are stabilized by interadsorbate interactions. The binding energy differs considerably for HBE molecules depending on local configuration, and our calculations do not reproduce these as being more stable than the LBE-h molecules. We deem it likely that, from a computational perspective, larger supercells are required to reproduce island configurations that give higher adsorption energies than that calculated for the isolated LBE-h molecules. We have investigated the effect of van der Waals (vdW) interactions by calculating energy corrections (not shown) to the RPBE values (see Theory section) for selected configurations and find that trends in the relative stability among HBE configurations and also compared with LBE molecules do not change.

Cyclotrimerization. Additional information can be obtained from the full temperature dependence of the SFG spectra. In Figure 4, temperature-programmed desorption of reactively formed benzene measured at mass 78 amu (TPR) is shown together with the corresponding SFG spectra. The sample was heated at a constant rate of 0.4 K/s during the experiment. The TPR trace shows a maximum in the benzene desorption rate at 305 K. This temperature is lower than the previously published temperature-programmed reaction experiments of C_2H_2 cyclotrimerization on Cu(110),[1,2] where the desorption maximum was found around 325 K. We attribute this difference to the different ramping rates, which was 3−6 K/s in previous experiments.

The left panel of Figure 4 shows a false-color plot of the SFG spectra as a function of temperature, where light parts indicate more intensity. Sum-frequency generation spectra were recorded during the heating with a temperature change of 3 K during each spectrum. In the right panel, spectra at some selected temperatures are shown. Resonance frequencies and amplitudes that were fitted using the temperature-dependent SFG spectra are shown in the top and bottom panels of Figure 5. We choose to plot the fitted amplitude rather than its square, which corresponds to the SFG intensity, since the amplitude is proportional to adsorbate coverage, given a constant cross-

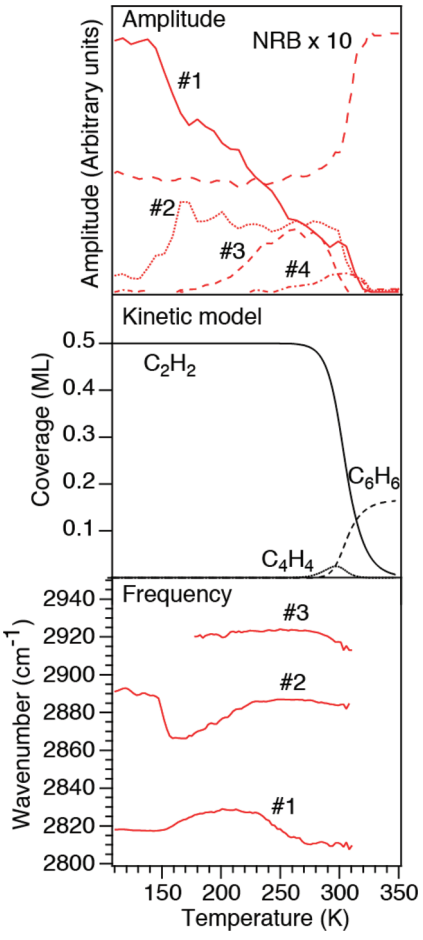

Figure 5. Top: Amplitudes for the nonresonant background (NRB) together with the four observed SFG resonances in order of increasing frequency. Middle: Temperature-dependent coverages of all species, obtained from kinetic modeling. Bottom: Frequencies obtained from curve fits for resonances 1−3 as a function of temperature.

section.[38] As in Figure 1, two peaks (#1 and #2) are observed at low temperature, with frequencies 2821 and 2896 cm^{-1}, respectively. Upon heating we observe intensity appearing around 2870 cm^{-1} between 150 and 160 K, which is correlated with decreased intensity in peak #1. This shows up in the curve fit as an increased amplitude and shift of resonance #2. We

dx.doi.org/10.1021/jp300514f | J. Phys. Chem. C 2012, 116, 9550−9560

interpret this as being due to molecules moving from one site to another, in agreement with previous XPS data.[25]

The transition at a temperature between 150 and 160 K at a heating rate of 0.4 K/s was modeled as a first-order reaction with barrier 0.45 ± 0.03 eV = 43 ± 3 kJ/mol assuming a typical attempt rate 10^{12}–10^{14} s^{-1}. This correlates perfectly with the loss of long-range order, which we measure by LEED, around 167 K when the sample is heated at 1.6 K/s. The computed activation barrier for diffusion correlates well with the experimental finding. Assuming a diffusion path starting in the hollow site, passing the long-bridge along the [1-10] direction into the adjacent hollow, a scenario also discussed by Kumagai et al.,[26] we obtain a barrier of 0.41 eV, i.e., 39.5 kJ/mol independent of coverage. According to STM and IETS,[26] the second site has to be stabilized by interadsorbate interactions, and we thus interpret this as the onset of diffusion leading to formation of molecular islands. The diffusion barrier is then slightly lower for C_2H_2 on Cu(110) than on Cu(100), where the barrier was determined to 0.53 eV with an attempt rate of $10^{13.6}$ s^{-1}.[51]

Around 180 K resonance #3 starts appearing at 2926 cm^{-1}. The amplitude of this resonance increases until its maximum at 265 K, where it is equal to the intensity of resonance #2. The appearance of resonance #3 is accompanied by a blue-shift of resonance #2, which is complete at 250 K, where the resonance appears at 2891 cm^{-1}. We interpret this as formation of larger islands where the adsorbate–adsorbate interaction is strong enough to create the asymmetrically adsorbed species that is observed in our SFG and previous XAS data.[25]

Above 255 K a resonance (#4) appears at 2960 cm^{-1}. The amplitude of this resonance increases until 300 K, where it reaches a plateau which persists until 315 K. This resonance is visible until 324 K and is the only resonance that we can resolve above 315 K. This temperature range is the same as where we observe benzene desorption in our TPR (see Figure 4) and makes it likely that this species is directly related to the cyclotrimerization reaction. Candidates would be adsorbed C_4H_4 or C_6H_6.

Adsorbed C_6H_6 is not readily observable with SFG due to the flat-lying geometry.[52] It is in principle symmetry-allowed because of the slightly tilted C–H bonds,[24,52] but the SFG signal can be expected to be weak. Figure 6 shows the temperature-dependent SFG recorded during heating of 3 monolayers of C_6H_6/Cu(110) with a linear ramp of 20 K/min. At low temperature, two sharp resonances are observed at 3036 and 3056 cm^{-1}, which we assign to second-layer adsorbed benzene. These resonances are red-shifted by 10 cm^{-1} compared to the C–H stretch resonances observed by Haq and King[53] at 3042, 3066, and 3084 cm^{-1} for two adsorbed C_6H_6 layers. These sharp resonances disappear simultaneously between 145 and 153 K, which correlates with the desorption temperature of the second adsorbed layer, where benzene molecules are well ordered standing edge-on at the surface.[54] The two sharp resonances are thus assigned to C–H stretch resonances of the second-layer benzene at the surface. As expected, no statistically significant C–H stretch resonance can be observed from the first layer in the present data. The resonance observed at 2960 cm^{-1} during the cyclotrimerization reaction must thus originate from another adsorbed species.

The previously proposed tilted C_4H_4 intermediate species[2] should be observable with SFG and can provide a plausible candidate for the origin of the observed resonance, provided that the surface coverage of the intermediate species is high enough during the reaction.

To study the proposed intermediate, we prepared C_4H_4 on Cu(110) by dissociation of $C_4H_4Cl_2$ according to the recipe given by Lomas et al.[2] As shown in Figure 7, this species gives a rather strong resonance at 2960 cm^{-1} at low coverage, shifting

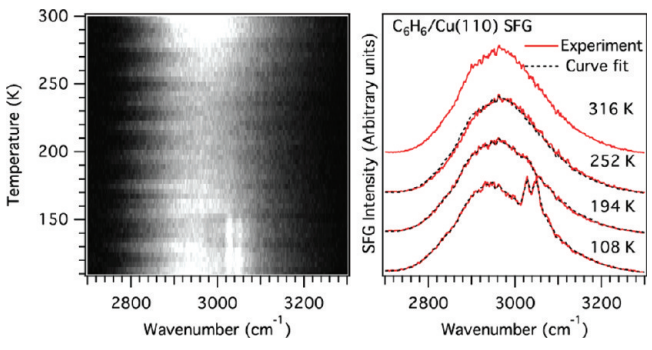

Figure 6. Temperature dependence of adsorbed C_6H_6. The left panel shows the experimental data as a false color plot, where dark denotes low intensity and light denotes high intensity. The right panel shows slices around a few temperatures.

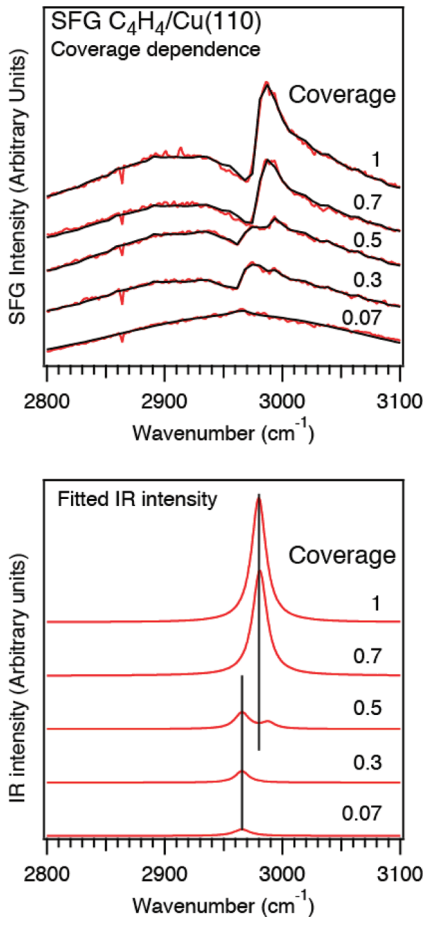

Figure 7. Coverage dependence of adsorbed C_4H_4. The top panel shows the experimental data together with curve fits. In the lower panel the resonances from the curve fits were scaled to correspond to the IR absorption. At low coverage a resonance at 2960 cm^{-1} is observed. Upon increasing coverage, this resonance shifts to higher frequency. The coverages are stated in fractions of a saturated monolayer.

dx.doi.org/10.1021/jp300514f | J. Phys. Chem. C 2012, 116, 9550–9560

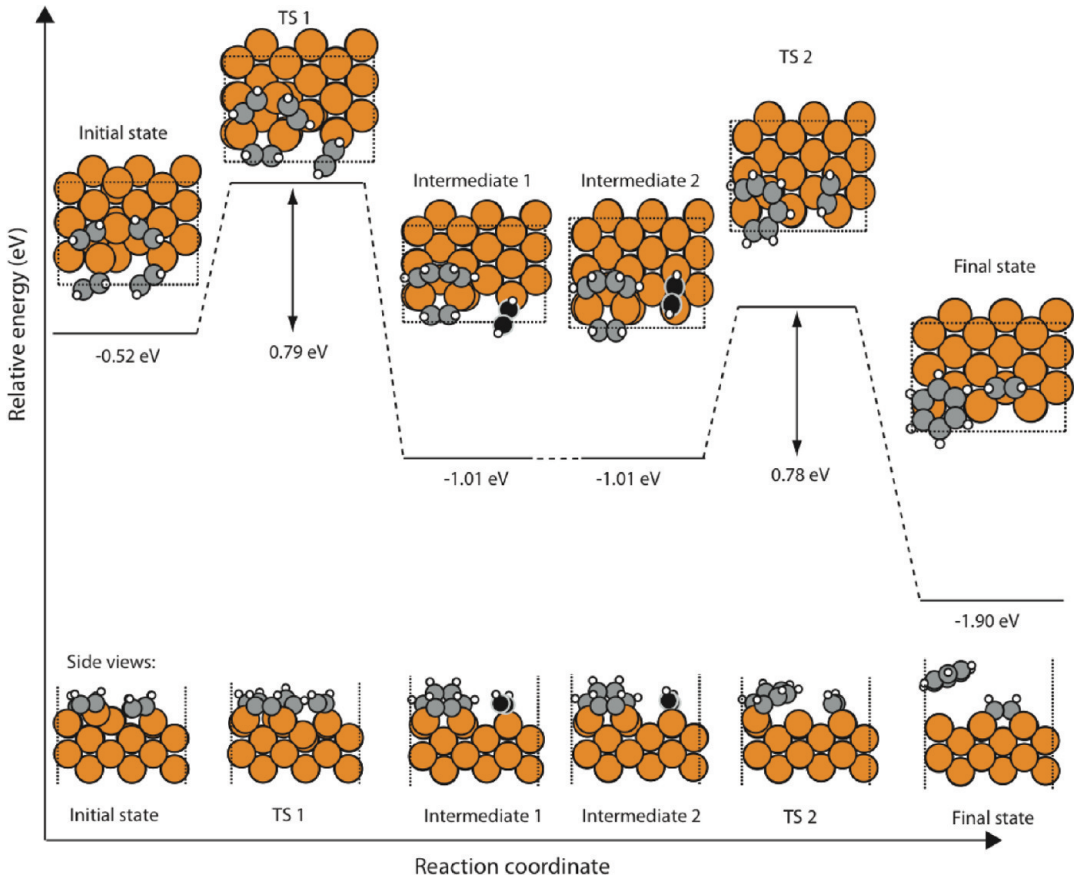

Figure 8. Potential energy surface of the cyclotrimerization of benzene on Cu(110) at a surface coverage of 0.44 ML with respect to acetylene. The initial state is taken as the reference state of the reaction when determining the activation barriers. The adsorption energy of the Initial state, Intermediate 1 and 2, and the Final state are referenced to the Cu slab and gas phase acetylene. Coordinates are available in the Supporting Information.

to 2975 cm^{-1} as the coverage is increased. This is in perfect agreement with the resonance observed during the cyclotrimerization reaction. Thus, we assign the resonance at 2960 cm^{-1} that we observe during the reaction to the C_4H_4 surface intermediate. We observe a single resonance from this species. Since it contains four C−H bonds one would expect at least two symmetry-allowed C−H stretch resonances unless all four C atoms are equivalent at the surface, which would suggest a flat-lying species. From the present data, however, we cannot rule out a weaker second resonance below our detection threshold and a tilted geometry as was found in the Pd(111) case, where this intermediate was investigated with XAS.[55] The resonance observed during the reaction does compare well with that of the adsorbed C_4H_4, and comparing the intensity of the fourth resonance in our temperature-dependent C_2H_2 SFG with that of the directly adsorbed C_4H_4 species, we estimate the maximum coverage of this species to be around 5−10% of saturation coverage during the reaction. This estimate is based on comparison with the fitted amplitude of the low-coverage resonance of the directly adsorbed C_4H_4, which was measured as a function of coverage, and the estimate that the saturation coverage of this species is at most 0.5 ML. This rather high surface concentration directly indicates that the barrier for benzene formation is of similar magnitude as the formation of the intermediate.

We can model the reaction using a kinetic model assuming a purely associative reaction in two steps with Arrhenius-like temperature dependence. The lack of coverage dependence in the cyclotrimerization reaction according to TPR data[2] suggests a pseudo first-order reaction,[56] although associative reactions are typically second-order. The lowering of the reaction order can be understood from the formation of densely packed islands, which in the ideal case makes the local C_2H_2 concentration independent of coverage. We modeled the first step of the reaction as zeroth- to second-order and the second step as first-order with respect to C_4H_4 and zeroth-order with respect to C_2H_2. Benzene is assumed to desorb without activation energy in the model. The free parameters in the model are the attempt rate and two activation barriers. We assume the same attempt rate for the different steps in the reaction and fit the modeled C_6H_6 desorption temperature, C_4H_4 surface concentration, and temperature dependence to the data obtained from our TPR and temperature-dependent SFG experiments.

Although we cannot determine the attempt rate directly from our SFG experiment, we can estimate the effective attempt rate for the total reaction based on our and previously published TPR data. The best fit to all available TPR data is obtained for an attempt rate of $10^{13\pm1}$ s^{-1}. Using this attempt rate to determine the reaction barriers from the SFG experiment, we arrive at a value of 84 ± 6 kJ/mol for the first step. The barrier of the second step is lower than the first by 5 ± 3 kJ/mol. An example of the resulting modeled coverages, of all three molecular species, is shown in the middle panel of Figure 5.

Figure 8 shows the corresponding calculated potential energy surface (PES) of the cyclotrimerization of benzene at a C_2H_2

dx.doi.org/10.1021/jp300514f | J. Phys. Chem. C 2012, 116, 9550−9560

coverage of 0.44 ML where the initial state of the reaction is constituted by molecules adsorbed asymmetrically in the hollow sites. The reaction proceeds via a C_4H_4 species adsorbed over the hollow site with a tilt away from the coadsorbed C_2H_2 molecule in the adjacent site in the [1-10] direction to minimize repulsion; if isolated at the surface, C_4H_4 stands up. To accurately reproduce the experimental estimates of the activation barriers in the cyclotrimerization, we assume an intermediate step in which a C_2H_2 molecule diffuses to an adjacent hollow site to maintain a local high coverage around the C_4H_4 species which affects the last step of the reaction, the trimerization step. To clarify, the C_2H_2 molecule colored black in the configuration denoted Intermediate 1 in Figure 8 diffuses along the [1-10] direction into the adjacent site, where it, due to repulsive interactions with the C_4H_4 species, moves closer toward the bridge site (see Intermediate 2). The justification of this process will be discussed further in the following. The final state of the cyclotrimerization, the adsorbed weakly bound C_6H_6 coadsorbed with two acetylene molecules, has a tilted (~20°) geometry relative the surface plane.

Isolating the benzene on the surface, i.e., a C_6H_6 surface coverage of 0.11 ML, reduces the tilt to ~2°. For this species, the adsorption energy is 0.12 eV, and the benzene is expected to desorb after it is formed, as also observed experimentally. At lower coverage, the adsorption energy of C_6H_6 was calculated to be 0.25 eV using the PBE XC-functional.[57] Recalculating our benzene structure using this XC-functional gives an adsorption energy of 0.17 eV which is slightly lower—an expected result since the coverage in our study is higher. A similar tilted, but more stable, configuration has been reported in previous studies[58] where the chemisorption energy was calculated to be 0.37 eV, also here using the PBE functional. Triguero et al.[24] modeled the system at a much lower coverage using a cluster approach and obtained a considerably stronger adsorbate–surface interaction (E_{ads} ~ 18 kcal/mol = 0.78 eV) for the quinoid structure of benzene. This, however, cannot be reproduced in the model system employed in the present study at 0.11 ML coverage with respect to C_6H_6. In fact, repeating the calculation with the same limited Cu_{13} cluster as was possible for Triguero et al.,[24] we confirm the quinoid structure, but this converts to the weakly bound C_6H_6 structure found in the present work upon extending the cluster size to Cu_{31} where all Cu atoms interacting with the adsorbate are coordinatively saturated; it is clear that in the small cluster the coordinatively unsaturated Cu atoms interacting with the two carbons in para-position had an artificially enhanced reactivity which stabilized the quinoid structure which experimentally is found only on more reactive transition metals.

We find a barrier for dimerization of C_2H_2 of 0.79 eV (76 kJ/mol) in good agreement with the experiment. At lower acetylene coverage, 0.33 ML, the barrier is 0.80 eV suggesting a small to insignificant dependence on the local coverage in this step. The second step of the reaction is found to be slightly less activated, as also seen experimentally, with a barrier for trimerization of 0.78 eV (75 kJ/mol), i.e., lower than the first step by 1 kJ/mol. The activation barrier for the trimerization step is highly dependent on the local coverage and configuration; at 0.33 ML with respect to acetylene the barrier was found to be 0.58 eV. The excellent agreement with experiment for the trimerization step is obtained by assuming a C_2H_2 molecule adsorbed in the adjacent site to the C_4H_4 species—the former molecule causing steric effects on the ring-closing mechanism and thus increasing the barrier. In the preceding step of the reaction, a C_2H_2 molecule participating in the dimerization occupies this site (Initial state in Figure 8), which suggests that a neighboring nonparticipating C_2H_2 may, as the site becomes free (Intermediate 1), diffuse into this site (Intermediate 2). This reasoning becomes justified by the fact that Intermediates 1 and 2 are iso-energetic, with an assumed low diffusion barrier.

We also investigated the effect of vdW interactions on the reactant and product states of the cyclotrimerization but found effects only on the order of 0.05 eV on the adsorption energies, suggesting that the effects on the barriers would likely be of similar magnitude.

In the case of cyclotrimerization of acetylene to benzene on Pd(111), the attempt rate and benzene formation barrier were determined experimentally using laser-induced thermal desorption.[59] An attempt rate of $10^{9.8}$ s^{-1} was found along with an activation barrier of 43.5 kJ/mol. The attempt rate we determine is significantly higher, but the reaction mechanism is different, and there is no reason to a priori assume similar attempt rates. The barriers are also higher on Cu(110), which is consistent with the fact that Cu is a noble metal, whereas Pd is a transition metal, which would be assumed to be more reactive. There are also differences due to the different exposed surface faces where a decrease in reactivity going from (111) surfaces to (110) surfaces is generally observed.[60] A connection can be made to the correlation between the metal d-band center and the adsorption energy of the reactants, in turn often associated with the reactivity; going from (111) to (110), the coordination number of the metal atoms decreases which is associated with an upshift of the d-band and hence an increased chemisorption energy for the adsorbates,[61] leading to a higher activation barrier.

Returning to the kinetic model, we note that the width of the benzene desorption peak and that of the intermediate are both broader in the experiment than in our model and assume that this is due to the assumption of a well-defined and coverage-independent attempt rate and barrier. In reality one can expect dependencies of these values on coverage through changes in adsorbate structure with coverage. In the present model benzene desorption is assumed to occur without activation energy. Indeed the computed energy for desorption 0.12 eV (11.7 kJ/mol) from the DFT calculations for isolated benzene molecules at 0.11 ML indicates that benzene will desorb as it is formed.

■ CONCLUSIONS

In conclusion, we have presented a consistent experimental and theoretical picture of the thermal evolution of adsorbed C_2H_2 at the Cu(110) surface and the cyclotrimerization to benzene. At low temperature, we find two adsorption sites, in agreement with previous experimental studies and supported by our calculations. The molecules move from one site to the other upon heating and subsequently form molecular islands consisting mainly of an asymmetrically adsorbed C_2H_2 species at the surface. We calculate chemisorption energies for a number of configurations containing acetylene species of this kind and find that adsorbate–adsorbate interactions are decisive for the stability of the local configurations. We find a computed activation barrier for the diffusion of ~40 kJ/mol in excellent agreement with the experimental 43 ± 1 kJ/mol. Around 300 K we observe adsorbed C_4H_4, which is the reaction intermediate in the cyclotrimerization reaction of acetylene to benzene at Cu(110). We apply a kinetic model to the reaction

and conclude that formation of gas phase benzene proceeds in two steps, which can be successfully modeled with an attempt rate of $10^{13\pm1}$ s^{-1}: a barrier for formation of the C_4H_4 intermediate of 84 ± 6 kJ/mol and a barrier for benzene formation, which is lower by 5 ± 3 kJ/mol. The cyclotrimerization reaction is also modeled by means of DFT with excellent agreement for both activation barriers.

■ ASSOCIATED CONTENT

Supporting Information

Coordinates to the structures reported in Figures 3 and 8. This material is available free of charge via the Internet at http://pubs.acs.org.

■ AUTHOR INFORMATION

Corresponding Author

*E-mail: ostrom@fysik.su.se. Phone: +46-8-5537 8641. Fax: +46-8-5537 8601.

Notes

The authors declare no competing financial interest.

■ ACKNOWLEDGMENTS

We acknowledge the Swedish Research Council for financial support. The DFT calculations were performed on resources provided by the Swedish National Infrastructure for Computing (SNIC) at the LUNARC center and the High Performance Computing Center North.

■ REFERENCES

(1) Avery, N. R. *J. Am. Chem. Soc.* **1985**, *107*, 6711−6712.
(2) Lomas, J. R.; Baddeley, C. J.; Tikhov, M. S.; Lambert, R. M. *Langmuir* **1995**, *11*, 3048−3053.
(3) Dvorak, J.; Hrbek, J. *J. Phys. Chem. B* **1998**, *102*, 9443−9450.
(4) Kyriakou, G.; Kim, J.; Tikhov, M. S.; Macleod, N.; Lambert, R. M. *J. Phys. Chem. B* **2005**, *109*, 10952−10956.
(5) Baddeley, C. J.; Ormerod, R. M.; Stephenson, A. W.; Lambert, R. M. *J. Phys. Chem.* **1995**, *99*, 5146.
(6) Baddeley, C. J.; Tikhov, M.; Hardacre, C.; Lomas, J. R.; Lambert, R. M. *J. Phys. Chem.* **1996**, *100*, 2189−2194.
(7) Lee, A. F.; Baddeley, C. J.; Lambert, R. M. *J. Phys. Chem. B* **1997**, *101*, 2797.
(8) Lusvardi, V. S.; Pierce, K. G.; Barteau, M. A. *J. Vac. Sci. Technol. A* **1997**, *15*, 1586.
(9) Ormerod, R. M.; Lambert, R. M. *Catal. Lett.* **1990**, *6*, 121.
(10) Pierce, K. G.; Barteau, M. A. *J. Phys. Chem.* **1994**, *98*, 3882.
(11) Tysoe, W. T.; Nyberg, G. L.; Lambert, R. M. *Surf. Sci.* **1983**, *135*, 128−146.
(12) Xu, C.; Peck, J. W.; Koel, B. E. *J. Am. Chem. Soc.* **1993**, *115*, 751.
(13) Pacchioni, G.; Lambert, R. M. *Surf. Sci.* **1994**, *304*, 208−222.
(14) Chatt, J.; Duncanson, L. A. *J. Chem. Soc.* **1953**, 2939.
(15) Dewar, M. J. S. *Bull. Soc. Chim. Fr.* **1951**, *18*, C79.
(16) Arvanitis, D.; Wenzel, L.; Baberschke, K. *Phys. Rev. Lett.* **1987**, *59*, 2435.
(17) Bao, S.; Hofmann, P.; Schindler, K.-M.; Fritsche, V.; Bradshaw, A. M.; Woodruff, D. P.; Casado, C.; Asensio, M. C. *Surf. Sci.* **1994**, *307*−*309*, 722−727.
(18) Bao, S.; Hofmann, P.; Schindler, K.-M.; Fritzsche, V.; Bradshaw, A. M.; Woodruff, D. P.; Casado, C.; Asensio, M. C. *J. Phys.: Condens. Matter* **1994**, *6*, L93−L98.
(19) Bao, S.; Hofmann, P.; Schindler, K.-M.; Fritzsche, V.; Bradshaw, A. M.; Woodruff, D. P.; Casado, C.; Asensio, M. C. *Surf. Sci.* **1995**, *323*, 19−29.
(20) Fuhrmann, D.; Wacker, D.; Weiss, K.; Hermann, K.; Witko, M.; Wöll, C. *J. Chem. Phys.* **1998**, *108*, 2651.
(21) Hermann, K.; Witko, M. *Surf. Sci.* **1995**, *337*, 205−214.
(22) Hermann, K.; Witko, M. *J. Mol. Struct. (Theochem)* **1999**, *458*, 81−92.
(23) Lomas, J. R.; Baddeley, C. J.; Tikhov, M. S.; Lambert, R. M.; Pacchioni, G. *Langmuir* **1997**, *13*, 758−764.
(24) Triguero, L.; Pettersson, L. G. M.; Minaev, B.; Ågren, H. *J. Chem. Phys.* **1998**, *108*, 1193.
(25) Öström, H.; Nordlund, D.; Ogasawara, H.; Weiss, K.; Triguero, L.; Pettersson, L. G. M.; Nilsson, A. *Surf. Sci.* **2004**, *565*, 206−222.
(26) Kumagai, T.; Hatta, S.; Okuyama, H.; Aruga, T. *J. Chem. Phys.* **2007**, *126*, 234708.
(27) Pettersson, L. G. M.; Ågren, H.; Luo, Y.; Triguero, L. *Surf. Sci.* **1998**, *408*, 1.
(28) Haq, S.; Laroze, S. C.; Mitchell, C.; Winterton, N.; Raval, R. *Surf. Sci.* **2003**, *531*, 145−148.
(29) Haq, S.; Laroze, S. C.; Mitchell, C.; Winterton, N.; Raval, R. *J. Mol. Catal. A* **2009**, *305*, 117−120.
(30) Laroze, S. C.; Haq, S.; Raval, R.; Jugnet, Y.; Bertolini, J. C. *Surf. Sci.* **1999**, *433*−*435*, 193−198.
(31) Beernink, G.; Gunia, M.; Dötz, F.; Öström, H.; Weiss, K.; Müllen, K.; Wöll, C. *ChemPhysChem* **2001**, *2*, 317.
(32) Zhu, X. D.; Suhr, H.; Shen, Y. R. *Phys. Rev. B* **1987**, *35*, 3047.
(33) Richter, L. J.; Petralli-Mallow, T. P.; Stephenson, J. C. *Opt. Lett.* **1998**, *23*, 1594.
(34) Yang, M.; Chou, K. C.; Somorjai, G. A. *J. Phys. Chem. B* **2003**, *107*, 5267−5272.
(35) McCrea, K. R.; Somorjai, G. A. *J. Mol. Catal. A* **2000**, *163*, 43−53.
(36) Woodruff, D. P.; Hayden, B. E.; Prince, K.; Bradshaw, A. M. *Surf. Sci.* **1982**, *123*, 397−412.
(37) Harendt, C.; Goschnick, J.; Hirschwald, W. *Surf. Sci.* **1985**, *152*/*153*, 453−462.
(38) Shen, Y. R. *The principles of non-linear optics*; John Wiley & Sons Inc: New York, 1984.
(39) Hunt, J. H.; Guyot-Sionnest, P.; Shen, Y. R. *Chem. Phys. Lett.* **1987**, *133*, 189.
(40) Enkovaara, J.; et al. *J. Phys.: Condens. Matter* **2010**, *22*, 253202.
(41) Mortensen, J. J.; Hansen, H. A.; Jacobsen, K. W. *Phys. Rev. B* **2005**, *71*, 035109.
(42) Blöchl, P. E. *Phys. Rev. B* **1994**, *50*, 17953.
(43) Hammer, B.; Hansen, L. B.; Nørskov, J. K. *Phys. Rev. B* **1999**, *59*, 7413.
(44) Perdew, J. P.; Burke, K.; Ernzerhof, M. *Phys. Rev. Lett.* **1996**, *77*, 3865.
(45) Monkhorst, H. J.; Pack, J. D. *Phys. Rev. B* **1976**, *13*, 5188−5192.
(46) Henkelman, G.; Uberuaga, B. P.; Jónsson, H. *J. Chem. Phys.* **2000**, *113*, 9901.
(47) Román-Pérez, G.; Soler, J. M. *Phys. Rev. Lett.* **2009**, *103*, 096102.
(48) Dion, M.; Rydberg, H.; Schröder, E.; Langreth, D. C.; Lundqvist, B. I. *Phys. Rev. Lett.* **2004**, 92.
(49) Dion, M.; Rydberg, H.; Schröder, E.; Langreth, D. C.; Lundqvist, B. I. *Phys. Rev. Lett.* **2005**, *95*, 109902.
(50) Shimanouchi, T. *Molecular Vibrational Frequencies*; In NIST Chemistry WebBook, NIST Standard Reference Database Number 69; Linstrom, P. J., Mallard, W. G., Eds.; National Institute of Standards and Technology: Gaithersburg, MD; http://webbook.nist.gov; (accessed Nov 8, 2011).
(51) Lauhon, L. J.; Ho, W. *J. Chem. Phys.* **1999**, *111*, 5633.
(52) Weinelt, M.; Wassdahl, N.; Wiell, T.; Karis, O.; Hasselström, J.; Bennich, P.; Nilsson, A. *Phys. Rev. B* **1998**, *58*, 7351.
(53) Haq, S.; King, D. *J. Phys. Chem.* **1996**, *100*, 16957−16965.
(54) Lee, J.; Dougherty, D. B.; John T. Yates, J. *J. Phys. Chem. B* **2006**, *110*, 15645−15659.
(55) Ormerod, R. M.; Lambert, R. M.; Hoffmann, H.; Zaera, F.; Yao, J. M.; Saldin, D. K.; Wang, L. P.; Bennett, D. W.; Tysoe, W. T. *Surf. Sci.* **1993**, *295*, 277−286.
(56) Redhead, P. A. *Vacuum* **1962**, *12*, 203.
(57) Atodiresei, N.; Caciuc, V.; Lazić, P.; Blügel, S. *Phys. Rev. Lett.* **2009**, *102*, 136809.

(58) Lesnard, H.; Lorente, N.; Bocquet, M.-L. *J. Phys.: Condens. Matter* **2008**, *20*, 224012.
(59) Abdelrehim, I. M.; Thornburg, N. A.; Sloan, J. T.; Caldwell, T. E.; Land, D. P. *J. Am. Chem. Soc.* **1995**, *117*, 9509−9514.
(60) Mavrikakis, M.; Hammer, B.; Nørskov, J. K. *Phys. Rev. Lett.* **1998**, *81*, 2819.
(61) Ge, Q.; Neurock, M. *Chem. Phys. Lett.* **2002**, *358*, 377.